Eur Respir J 1998; 12: 170–176
DOI: 10.1183/09031936.98.12010170

European Respiratory Journal
ISSN 0903 - 1936

Respiratory mechanics in ventilated COPD patients: forced oscillation *versus* occlusion techniques

R. Farré*, M. Ferrer+, M. Rotger*, A. Torres+, D. Navajas*

Respiratory mechanics in ventilated COPD patients: forced oscillation versus *occlusion techniques. R. Farré, M. Ferrer, M. Rotger, A. Torres, D. Navajas. ©ERS Journals Ltd 1998.*

ABSTRACT: The respiratory mechanics of artificially ventilated chronic obstructive pulmonary disease (COPD) patients were investigated by means of the forced oscillation (FOT) and the end-inspiratory airway occlusion (AOT) techniques.

FOT was applied to measure respiratory resistance (R_{rs}) and reactance (X_{rs}) from 0.25–16 Hz. Maximum (R_{max}) and minimum (R_{min}) resistances, static elastance (E_{st}) and time constant (τ) were computed by AOT. FOT and AOT data were interpreted with models featuring airway wall shunt, tissue viscoelasticity and parallel inhomogeneity. R_{rs}* and X_{rs}*, predicted from the AOT data, were computed and compared with R_{rs} and X_{rs} measured by FOT.

R_{rs} and X_{rs} (hPa·s·L^{-1}) decreased from 31.2±10.3 to 5.9±4.6 and increased from -20.3±7.1 to -8.0±4.4 from 0.25–16 Hz, respectively. Central resistance (R_c) and peripheral resistance (R_p) (in hPa·s·L^{-1}), and shunt elastance (E_{sh}) and tissue elastance (E_t) (in hPa·L^{-1}) were 4.4±5.4, 28.4±15.3, 723±393 and 31.8±10.1, respectively. R_{min}, R_{max} and E_{st} were 18.4±5.9, 28.4±12.8 and 18.1±4.2 respectively, and τ=0.76±0.25 s. The frequency dependence of predicted R_{rs}* and X_{rs}* differed markedly from that of measured R_{rs} and X_{rs}.

The use of different models to interpret the measured data suggests that both airway and tissue properties determined the frequency dependence of respiratory resistance and respiratory reactance in ventilated chronic obstructive pulmonary disease patients at the investigated frequencies (0.25–16 Hz).
Eur Respir J 1998; 12: 170–176.

*Laboratory Biofisica i Bioenginyeria, Facultat de Medicina, IDIBAPS, Universitat de Barcelona, Spain. +Servei de Pneumologia, Hospital Clinic Provincial de Barcelona, IDIBAPS, Barcelona, Spain.

Correspondence: R. Farré
Laboratory Biofisica i Bioenginyeria
Facultat de Medicina
Casanova 143
E-08036 Barcelona
Spain
Fax: 34 3 4035260

Keywords: Airway resistance
frequency dependence
lung inhomogeneity
monitoring
respiratory impedance
viscoelasticity

Received: July 28 1997
Accepted after revision March 13 1998

This work was supported in part by Comisión Interministerial de Ciencia y Tecnología (CICYT, SAF96-0076)

Optimization of the ventilator settings in mechanical ventilation is a key issue in minimizing the risk of barotrauma and haemodynamic compromise, in avoiding hyperinflation and in reducing the work of breathing [1]. Improvement in the ventilator variables may be facilitated by better understanding of the role played by the different mechanical properties of airways and tissue in determining the dynamic relationships among the pressure, flow and volume excursions applied to the patient's respiratory system [2, 3]. The use of a mechanical model to mimic respiratory mechanics as realistically as possible for each pathological situation may be helpful in predicting the outcome variables of clinical interest in response to the applied ventilator waveform. In the case of mechanically ventilated chronic obstructive pulmonary disease (COPD) patients, the conventional simple model consisting of a resistance and an elastance is not able to describe adequately the behaviour of the respiratory system [4]. In these patients, respiratory mechanics has been interpreted in terms of the viscoelastic tissue properties and/or the gas redistribution phenomena due to airways inhomogeneity [5–7].

Published works devoted to analysing in detail the dynamic response of the respiratory system in artificially ventilated COPD patients report conflicting results. Indeed, when the technique of end-inspiratory airway occlusion with a constant flow inflation was applied, the effective resistance and elastance of the respiratory system could be interpreted in terms of a homogeneous resistance and a viscoelastic tissue compartment [5]. By contrast, data obtained by means of the forced oscillation technique (FOT) in COPD patients suggested that airway inhomogeneity plays a major role in determining the frequency dependence of respiratory resistance and reactance over a wide frequency range [7]. Nevertheless, it is difficult to compare the results from these works since the two techniques applied differ in both the frequency domain and the amplitude range of excursions and were applied to patients with possibly different degrees of COPD. Therefore, the aim of this work was to characterize better the mechanics of the respiratory system in artificially ventilated COPD patients by applying the FOT and the end-inspiratory airway occlusion technique (AOT) to the same patients. A key point in making the comparison between the two techniques was to extend the FOT measurements to the low frequencies typical of the occlusion technique. To this end, a modified FOT device [8] was used which, in contrast to the set-ups used in previous measurements in mechanically ventilated patients [7, 9], allowed FOT to be applied for frequencies down to 0.25 Hz. The results obtained by means of both techniques were interpreted in terms of models featuring tissue and airway properties.

Subjects and methods

The study was conducted on five (four males and one female) COPD patients who were admitted to the respiratory intensive care unit (ICU) of the hospital owing to an acute exacerbation of their underlying disease. The COPD diagnosis was established according to the forced expiration indices determined after or before the admission of the patient into the ICU. The study protocol was approved by the Ethics Committee of the hospital and informed consent was obtained from the next of kin of the patients. The study was carried out 12–36 h after the admission of the patient to the ICU. The patients, in a supine position and intubated with a cuffed orotracheal tube (8 mm internal diameter (ID)), were mechanically ventilated with a Siemens Servoventilator 900-C (Siemens, Solna, Sweden) in the constant flow volume-controlled mode. The ventilator settings (table 1) were established by the attending physician. To carry out the study, which lasted for ~20 min, the patients were sedated (*i.v.* infusion of 5–10 mg of midazolam, Dormicum®; Roche SA, Madrid, Spain) and paralysed (*i.v.* infusion of 2 mg of pancuronium bromide, Pavulon®; Orgenon-Hermes SA, Sant Boi de Llobregat, Spain). At the start of the study, tracheal secretions were conventionally aspirated and external positive end-expiratory pressure (PEEP), if any, was removed. The inflating pressure of the endotracheal tube cuff was checked periodically and care was taken to avoid leaks in the connections.

Flow was measured by means of a heated Fleisch-II type pneumotachograph (Metabo, Epalinges, Switzerland) placed between the Y-piece of the ventilator and the endotracheal tube. The pressure drop across the pneumotachograph was recorded with a differential transducer (±2 hPa, LCVR; Celesco, Canoga Park, CA, USA). Tracheal pressure was measured with a piezo-resistive pressure transducer (176PC/14; Honeywell, Freeport, IL, USA) connected to a catheter (50 cm in length and 0.12 cm ID) with a lateral pressure port at its tip placed 2 cm beyond the outlet of the endotracheal tube [10]. This catheter was periodically cleaned by injecting a bolus of 3 mL of air through it. Pressure and flow signals were low-pass filtered (Butterworth, eight poles, 32 Hz), sampled at 128 Hz and stored in a microcomputer. A FOT generator especially designed for low-frequency measurements in mechanically ventilated patients [8] was placed in parallel with the ventilator in the inspiratory line. The FOT generator was connected to the inspiratory line by means of a flexible tube (2 mm ID, 80 cm) and a Y-valve. This valve, which was closed during the normal ventilator cycling, was connected directly to the Y-piece to increase minimally the air volume, and hence the compliance, in the ventilation line when the valve was closed. The compliance of the system connecting the ventilator to the patient was decreased by omitting the humidifier and reducing the length of the standard low-compliance tubing of the ventilator (2 cm ID, 60 cm) [5]. Four end-inspiratory occlusion manoeuvres and four FOT measurements were carried out in a random order in each patient, allowing at least 10 normal ventilation cycles between measurements.

Table 1. – Ventilation parameters

Patient No.	f_B beats·min^{-1}	t_I s	V_T L	V' L·s^{-1}	F_{I,O_2}	PEEPi hPa
1	11.2	1.29	0.512	0.397	0.40	10.6
2	11.3	1.37	0.423	0.308	0.30	10.9
3	15.0	0.95	0.539	0.567	0.35	10.3
4	11.2	1.15	0.556	0.483	0.40	10.1
5	11.3	1.33	0.589	0.443	0.32	10.8
Mean	12.0	1.22	0.524	0.440	0.35	10.5
SD	1.7	0.17	0.063	0.097	0.05	0.3

f_B: ventilator frequency; t_I: inspiratory time; V_T: tidal volume; V': constant flow inflation; F_{I,O_2}: oxygen inspiratory fraction; PEEPi: intrinsic positive end-expiratory pressure.

To measure respiratory system resistance (R_{rs}) and reactance (X_{rs}) by FOT the expiratory valve of the ventilator was occluded by pressing the corresponding button and the valve connecting the FOT generator to the patient was manually opened. The forced oscillation signal (±3 hPa, ±80 mL·s^{-1}) contained power at 0.25, 0.5, 1, 2, 4, 8 and 16 Hz and the amplitudes of the low-frequency components were enhanced. FOT was applied for ~12 s of end-expiratory pause at the intrinsic PEEP (PEEPi) corresponding to the ventilator settings in each patient (table 1). After application of FOT the normal ventilator cycle was resumed. R_{rs} and X_{rs} were computed from the last 8 s of the recorded pressure and flow. These signals were divided into three blocks of 4 s each (50% overlapping). After subtraction of the mean value, each block was multiplied by a Hanning window and its fast Fourier transform (FFT) was computed. R_{rs} and X_{rs} were computed by averaging in the frequency domain (12 blocks) the data from the four FOT measurements. The frequency responses of the pressure and flow measuring systems were digitally corrected.

The end-inspiratory occlusion manoeuvre was applied first by pushing (~3 s) the end-expiratory button of the ventilator to reach PEEPi, then by releasing the hold button to allow for the inspiratory inflation and then by pressing the end-inspiratory pause button for ~6 s before resuming normal ventilation [5, 11–13]. For each occlusion manoeuvre the closing time was defined as the time at which flow decreased by 50%. The four occlusion manoeuvres in each patient were averaged after being synchronized in accordance with the closing time. The effect of the finite closure time of the ventilator valve was reduced as suggested [14]. Pressure immediately before flow interruption (P_1) was determined by extrapolating the preocclusion increasing pressure to the closing time. Pressure immediately after flow interruption (P_2) was determined by backextrapolation of the postocclusion decreasing pressure to the closing time. The plateau pressure at 3 s after the occlusion (P_3) and the time constant (τ) of the pressure relaxation immediately after the flow interruption were computed. The resistances and elastances commonly used to characterize the occlusion manoeuvre were computed as $R_{min}=(P_1-P_2)/V'$, $R_{max}=(P_1-P_3)/V'$, $E_{st}=(P_3-PEEP_i)/V_T$ and $\Delta E=(P_2-P_1)V_T$ [5, 11–13], where R_{min} = minimum resistance, R_{max} = maximum resistance, V' = gas flow, E_{st} = static elastance, V_T = tidal volume, and ΔE = differences in elastance.

Data measured by FOT and by the occlusion technique were interpreted in terms of the models A, B and C in figure 1. Model A, which was initially proposed by MEAD [15] and recently used to interpret FOT data in ventilat- ed COPD patients [7], consists of a central resistance (R_c), a shunt elastance (E_{sh}) accounting for airway wall compliance, a peripheral resistance (R_p) and a tissue elastance (E_t). Model B, usually employed to interpret respiratory

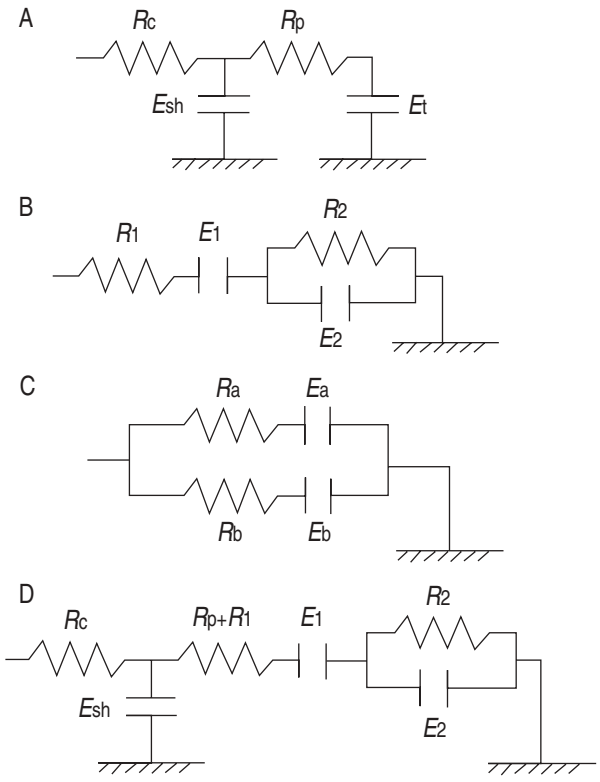

Fig. 1. – Mechanical models to interpret data measured by the forced oscillation and airway occlusion techniques. A: Central (Rc) and peripheral (Rp) airway resistances, shunt (Esh) and tissue (Et) elastances. B: Airway resistance (R1) and viscoelastic tissue compartment (E1, R2, E2). C: Inhomogeneous parallel (Ra-Ea and Rb-Eb) pathways. D: Central (Rc) and peripheral (Rp) airway resistances, airway shunt elastance (Esh), Newtonian tissue resistance (R1) and viscoelastic tissue compartment (E1, R2, E2).

system mechanics by means of the occlusion technique [16], consists of an airway resistance (R1) and a viscoelastic compartment of the respiratory tissues (R2, E1 and E2). Model C corresponds to a respiratory system inhomogeneity characterized by two parallel resistance-elastance (Ra-Ea, Rb-Eb) pathways. The concept of parallel inhomogeneity was initially proposed by Otis *et al*. [17] and has more recently been employed to interpret the frequency dependence of resistance and elastance [18–20]. As these models (A, B and C) are described by the same general equation of motion, they exhibit the same frequency dependence of resistance and reactance and the same response when subjected to the occlusion manoeuvre [6, 21]. Consequently, the parameters of one of the models can be computed from the parameters of any of the other models. Rrs and Xrs measured by FOT were used to compute the Rc, Esh, Rp and Et of model A by minimizing the distance (ε) between the model and the data [7] for positive values of the parameters. R1, E1, R2 and E2 of model B and Ra, Ea, Rb and Eb of model C were computed from the parameters derived from model A. The data obtained by the occlusion technique were used to compute the parameters R1, R2, E1 and E2 of model B ($R1=R\text{min}$, $E1=E\text{st}$, $R2=(R\text{max}-R\text{min})/(1-\exp(-t1/\tau))$ and $E2=R2/\tau$ [5, 11–13, 21–23]) and these values were used to compute Rc, Esh, Rp and Et of model A and Ra, Ea, Rb and Eb of model C. The frequency dependence of respiratory resistance (Rrs*) and reactance (Xrs*) estimated for each patient from the occlusion technique was computed ($R\text{rs}^*=R1+R2/(1+(2\pi f\tau)^2)$ and $X\text{rs}^*=E\text{st}-2\pi f\tau^2 E2/(1+(2\pi f\tau)^2)$ [21]).

In addition to the simple models A, B and C, Rrs, and Xrs, measured by FOT were interpreted by a more general model (fig. 1D) which includes compliant airways and a viscoelastic tissue compartment. The airway compartment consisted of Rc and Rp separated by Esh, as in model A. The tissue compartment was characterized by a Newtonian tissue resistance (R1), an elastance (E1) and an element with a time constant ($R2/E2$), as in model B. In this model, R1 and Rp play the same role in determining its mechanical properties and are, therefore, indistinguishable.

Results

Figure 2a plots the Rrs and Xrs from 0.25–16 Hz measured by FOT in a representative patient (no. 1). Figure 3a shows that, on average, Rrs (mean±SE) decreased progressively over the frequency bands from 31.2±4.6 hPa·s·L^{-1} at 0.25 Hz to 5.9±2.1 hPa·s·L^{-1} at 16 Hz. Xrs (mean±SE) increased markedly from -20.3±3.2 hPa·s·L^{-1} at 0.25 Hz to -10.1±1.8 hPa·s·L^{-1} at 2 Hz and from then on slightly increased to -8.0±2.0 hPa·s·L^{-1} at 16 Hz. Respiratory elastance (Ers; $E\text{rs}=-2\pi f\cdot X\text{rs}$) increased progressively with frequency in all patients (fig. 4). The use of models A, B and C to interpret the measured Rrs and Xrs resulted in

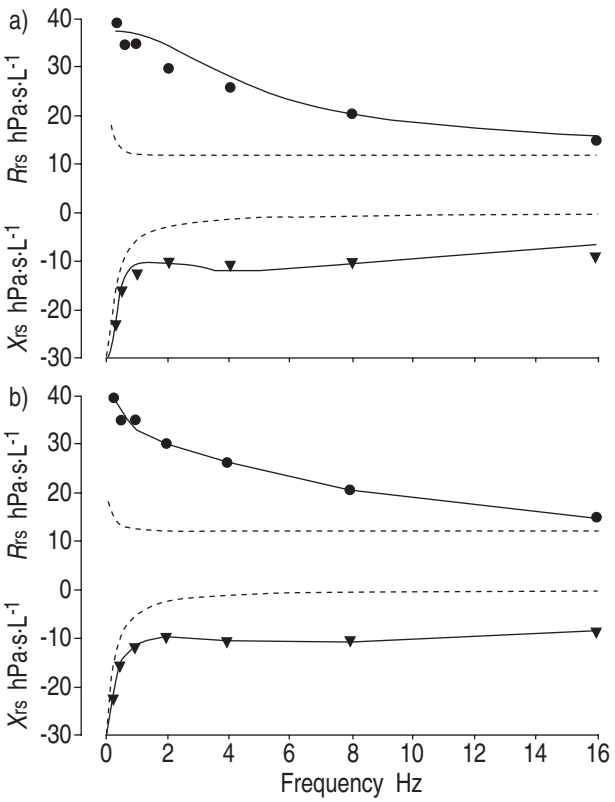

Fig. 2. – Example of the respiratory resistance (Rrs; ●) and reactance (Xrs; ▼) measured by the forced oscillation technique in patient no. 1. a) Solid lines correspond to fitting the equivalent models A, B or C in figure 1. b) Solid lines correspond to fitting model D in figure 1. Dashed lines in a) and b) correspond to respiratory resistance Rrs* and reactance Xrs* derived from the occlusion technique data in this patient.

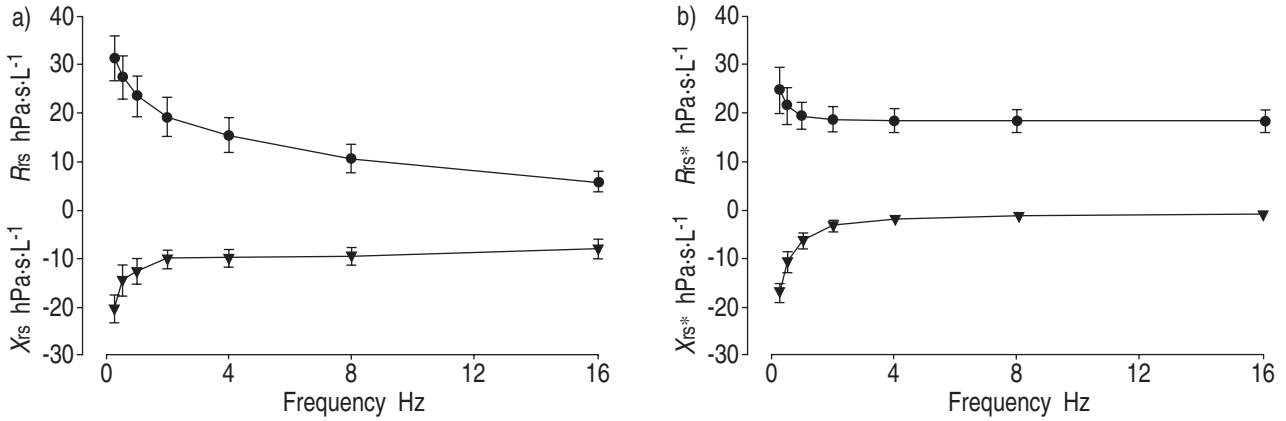

Fig. 3. – a) Respiratory resistance (*R*rs; ●) and reactance (*X*rs; ▼) measured by the forced oscillation technique. b) *R*rs* (●) and *X*rs* (▼) derived from the airway occlusion technique data. Values are shown as mean±SE.

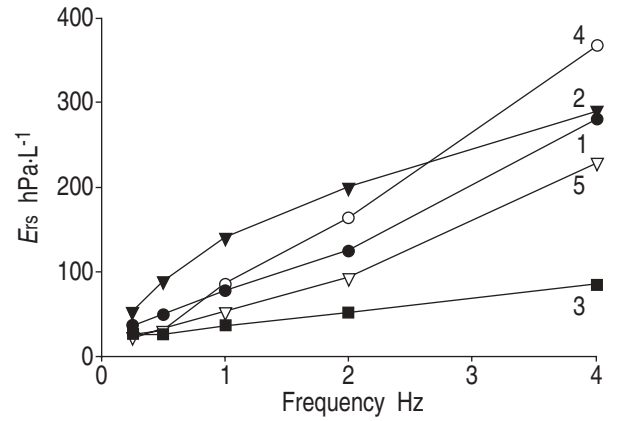

Fig. 4. – Frequency dependance of respiratory elastance (*E*rs) measured by forced oscillation technique in the five patients with chronic obstructive pulmonary disease. Labels indicate the patient number.

the parameters shown in table 2. The quality of the fit achieved (ε) is shown in table 2 and is illustrated in the representative example of figure 2a. The use of the more complex model D to fit the *R*rs and *X*rs measured by FOT resulted in the parameter values shown in table 3. This model was able to fit the data better than models A, B and C: on average, the fitting error ε decreased markedly from 2.35 hPa·s·L^{-1} (table 2, fig. 2a) to 0.83 hPa·s·L^{-1} (table 3, fig. 2b).

Table 3. – Resistances and elastances derived by fitting model D of figure 1 to forced oscillation technique data

Patient No.	ε	*R*c	*E*sh	*R*p+*R*1	*E*1	*R*2	*E*2
1	1.02	10.6	1040	22.1	29.8	9.5	40.9
2	0.53	2.14	374	29.5	38.2	20.4	119
3	0.64	0.0	875	10.7	29.8	36.5	25.5
4	1.57	0.0	1700	32.0	22.7	9.8	72.0
5	0.37	0.0	594	17.8	15.4	6.4	25.7
Mean	0.83	2.55	917	22.4	27.2	16.5	35.2
SD	0.48	4.60	507	8.7	8.6	12.4	23.0

Resistances are in hPa·s·L^{-1} and elastances in hPa·L^{-1}. ε (in hPa·s·L^{-1}): fitting error. See figure 1 for definitions of resistances and reactances.

The values of the resistances (*R*min, *R*max) and elastances (*E*st, Δ*E*) describing the end-inspiratory occlusion manoeuvre are shown in table 4. *R*max was systematically higher than *R*min and on average their difference (Δ*R*), which is an indirect index of the frequency dependence of resistance, was considerable: Δ*R*=10.0 hPa·s·L^{-1} (35% of *R*max). Δ*E* was systematically positive and on average was Δ*E*=8.0 hPa·L^{-1} (44% of *E*st). The time constant (τ) corresponding to the slow decrease in pressure after the airway occlusion was in the order of 1 s (0.76±0.25 s). The parameters of models A, B and C computed from the occlusion data are shown in table 5. *R*rs* and *X*rs* corresponding to the models (A, B and C) used to interpret the occlusion manoeuvres in patient no. 1 are shown in figure

Table 2. – Resistances and elastances derived by fitting models A, B and C of figure 1 to forced oscillation technique data

		Model											
		A				B				C			
Patient No.	ε	*R*c	*E*sh	*R*p	*E*t	*R*1	*E*1	*R*2	*E*2	*R*a	*E*a	*R*b	*E*b
1	2.59	13.6	702	24.0	42.2	13.6	39.8	21.4	662	23.3	1814	36.5	40.7
2	1.99	3.9	264	51.2	43.3	3.9	37.2	37.8	227	5.7	313	53.6	42.2
3	1.63	0.4	850	11.7	26.2	0.4	25.4	11.0	825	0.4	911	12.1	26.1
4	3.78	3.3	1305	35.2	25.4	3.3	24.9	33.9	1280	3.7	1566	38.4	25.3
5	1.76	0.8	496	20.0	21.9	0.8	21.0	18.3	475	0.9	538	20.7	21.8
Mean	2.35	4.4	723	28.4	31.8	4.4	29.7	24.5	694	6.8	1029	32.3	31.2
SD	0.88	5.4	393	15.3	10.1	5.4	8.3	11.1	396	9.5	647	16.2	9.5

Resistances are in hPa·s·L^{-1} and elastances in hPa·L^{-1}. ε (in hPa·s·L^{-1}): fitting error. See figure 1 for definitions of resistances and reactances.

Table 4. – Resistances, elastances and time constant from the end-inspiratory occlusion manoeuvres

Patient No.	R_{min} hPa·s·L^{-1}	R_{max} hPa·s·L^{-1}	E_{st} hPa·L^{-1}	ΔE hPa·L^{-1}	τ s
1	11.7	18.1	22.7	5.0	0.77
2	23.9	50.0	21.1	19.0	0.34
3	12.6	19.6	12.2	7.4	0.98
4	20.2	25.7	18.4	4.8	0.91
5	23.8	28.8	16.1	3.7	0.81
Mean	18.4	28.4	18.1	8.0	0.76
SD	5.9	12.8	4.2	6.3	0.25

R_{min}: minimum resistance; R_{max}: maximum resistance; E_{st}: static elastance; ΔE: change in elastance; τ: time constant.

2 (dashed lines). The mean±SE of R_{rs}* and X_{rs}* corresponding to the models (A, B and C) used to interpret the occlusion manoeuvres are shown in figure 3b. On average, R_{rs}* decreased markedly with frequency from R_{max} at zero frequency to R_{min} at ~1 Hz and remained constant at higher frequencies. X_{rs}* exhibited the frequency-dependent pattern characteristic of an effective elastance which rapidly increased from the static value E_1 at zero frequency to about E_2 at ~1 Hz and then remained constant at this value at higher frequencies.

A considerable discrepancy was found when comparing the frequency dependence of R_{rs} and X_{rs} measured by FOT (fig. 3a) and that of R_{rs}* and X_{rs}* derived from the interpretation of the occlusion manoeuvres with models A, B or C (fig. 3b). At 0.25 Hz, the lowest frequency measured by FOT, R_{rs} and X_{rs} showed no significant differences (paired t-test at level p=0.05) with R_{rs}* and X_{rs}*, respectively: R_{rs}=31.3±5.2, R_{rs}*=24.9±5.3, X_{rs}=-20.3±3.5, X_{rs}*=-16.9±2.2 (in hPa·s·L^{-1}; mean±SE). Nevertheless, R_{rs}* and X_{rs}* differed markedly from R_{rs} and X_{rs} at higher frequencies (above ~1 Hz). Moreover, the effective elastance E_{rs} measured by FOT (fig. 4) progressively increased with frequency while respiratory system elastance corresponding to the fitted models A, B and C increased up to ~1 Hz and from then on remained almost constant. Similarly, the parameters obtained when using models A, B or C to interpret FOT data (table 2) and occlusion technique data (table 5) were markedly different. This is clearly indicated by the characteristic time constant of the models: $R_p/(E_{sh}+E_t)$, R_2/E_2 and $(R_a+R_b)/(E_a+E_b)$ for models A, B and C, respectively [21]. Data from FOT resulted in parameter sets accounting for a time constant of ~35 ms, whereas the analysis of the occlusion manoeuvre data resulted in parameter sets for models A, B and C accounting for a much greater time constant of ~0.8 s.

Discussion

The first result obtained when applying FOT to mechanically ventilated COPD patients over a frequency band extending down to spontaneous breathing rates was that R_{rs} and X_{rs} exhibited a marked frequency dependence from 0.25–16 Hz. The second finding was that interpretation of FOT and occlusion technique data with the most common simple models used in the literature (A, B and C in fig. 1) provided conflicting results in terms of the parameter values (tables 2 and 5) and the frequency dependence of resistance and reactance (fig. 3). Such a result contrasts with data previously obtained in healthy dogs [16, 24] and in a series of patients including a minority with COPD [9], where both techniques provided consistent results. A possible reason for these results could be that simple models such as A, B and C featuring only one mechanism, *i.e.* airway wall shunting A, tissue viscoelasticity B, parallel inhomogeneity C, are not adequate to account for the dynamic response (0.25–16 Hz) of the respiratory system in mechanically ventilated COPD patients. In fact, a model (D in fig. 1) including two mechanisms, *i.e.* airway wall shunting and tissue viscoelasticity, was better able to reproduce the frequency dependence of R_{rs} and X_{rs} measured by FOT (fig. 2).

To our knowledge, this is the first study in which FOT has been applied in mechanically ventilated COPD patients for a frequency band extending down to spontaneous breathing frequencies (0.25 Hz). On average, R_{rs} (fig. 3) exhibited considerably high values and a marked negative frequency dependence, which contrasts with those (6.2 hPa·s·L^{-1} at 0.25 Hz and 1.8 hPa·s·L^{-1} at 16 Hz) reported for the same frequency band in healthy, anaesthetized, paralysed patients [25]. The most remarkable feature of X_{rs} (fig. 3) was that it always remained negative and therefore no patient exhibited the resonant frequency within the investigated frequency band, which is also in contrast to the findings in healthy patients [25]. The only FOT data available on mechanically ventilated patients correspond to frequencies above 4–5 Hz [7, 9]. BEYDON *et al.* [9] reported a negative frequency dependence of R_{rs} (35% decrease from 4–16 Hz), which was smaller than that found in the present study (65% decrease) between these two relatively high frequencies. Nevertheless, data from these

Table 5. – Resistances and elastances derived by fitting models A, B and C of figure 1 to the occlusion manoeuvres data (table 4)

	Model											
	A				B				C			
Patient No.	R_c	E_{sh}	R_p	E_t	R_1	E_2	R_1	E_2	R_a	E_a	R_b	E_b
1	11.7	33.0	81.1	72.7	11.7	22.7	7.9	10.3	83.6	114	25.4	28.4
2	23.9	98.6	43.1	26.8	23.9	21.1	26.6	77.5	53.3	302	58.1	22.7
3	12.6	22.7	52.8	26.4	12.6	12.2	11.3	10.5	51.6	64.1	33.6	15.1
4	20.2	26.8	77.4	58.7	20.2	18.4	7.6	8.4	126	156	33.5	20.9
5	23.8	23.6	60.4	50.7	23.8	16.1	6.1	7.5	159	220	33.8	17.4
Mean	18.4	40.9	62.9	47.1	18.4	18.1	11.9	22.8	94.7	171	36.9	20.9
SD	5.9	32.5	16.1	20.2	5.9	4.2	8.4	30.6	44.7	92.7	12.4	5.1

Resistances are in hPa·s·L^{-1} and elastances in hPa·L^{-1}. See figure 1 for definitions of resistances and reactances.

authors were obtained from a population including few COPD patients (3 out of 16). By contrast, PESLIN *et al*. [7] reported data from a population of mechanically ventilated patients, most of whom (11 out of 17) suffered from COPD. These authors analysed respiratory mechanics at frequencies above 5 Hz during different phases of the ventilation cycle and reported a frequency dependence of R_{rs} and X_{rs} consistent with that found in the patients in this study [7]. The results obtained when using model A (table 2) indicate that the peripheral resistance R_p accounted for 87% of the total resistance (R_c+R_p) and the mean elas-tance E_{sh} partitioning central and peripheral resistances corresponded to a compliance of 1.4 mL·hPa^{-1}. This value was close to those reported by PESLIN *et al*. [7] (0.64–2.56 mL·hPa^{-1}) when using the same model to analyse FOT data in ventilated COPD patients from 5–20 Hz. Models B and C, which attribute the frequency dependence of R_{rs} to tissue viscoelasticity or to parallel inhomogeneity, respectively, resulted in a much lower time constant (~35 ms) than expected for these two mechanisms, which seem to determine the frequency dependence of R_{rs} mainly at the lowest frequencies [19, 20]. The fact that the frequency dependence of R_{rs} (fig. 3a) and E_{rs} (fig. 4) extends to frequencies >2 Hz suggests that the role played by airway wall shunting is not negligible [20].

The results obtained by means of the end-inspiratory AOT (table 4) were in keeping with the few data on COPD patients available in the literature. Resistances and elastances reported by POLESE *et al*. [5] were smaller than those in the present patients (by ~16% in E_{st}, and ΔE and by ~42% in R_{min} and R_{max}), probably owing to a greater severity in the obstructive pathology and/or a higher degree of hyperinflation in the patients in this study, as suggested by the fact that the measured $PEEP_i$ (table 1) was 44% greater than the value reported by POLESE *et al*. [5]. However, a remarkable agreement was found in the ratios R_{min}/R_{max} (0.64 from our data and 0.65 in [5]) and (E_{st}+ΔE)/E_{st} (0.70 both from our data and in [5]), which are representative of the frequency dependence of the respiratory system. The time constant τ ~0.8 s found in this study, which could not be compared with data on COPD patients since it was not reported in [5], was of the same order of magnitude, although smaller than in normal subjects (~1.3 s [11]). As expected, interpretation of the occlusion technique data with model B, which is commonly employed with this technique, provides tissue parameters (table 5) consistent with the values reported previously. From the results obtained by using model A, shunt elastance (E_{sh}) would be similar to tissue elastance (E_t) (table 5). According to the parameters for model C, the two parallel compartments would be characterized by time constants with a ratio, (R_a/E_a)/(R_b/E_b), of about 1/3. The more complex model D was not fitted to the occlusion data since the model interpretation of these data is limited by the relatively narrow effective band width of the signals recorded. Indeed, the occlusion technique, which is a forced excitation with a pulse of flow of ~1 s of duration, has its main frequency components restricted to the lowest frequencies (d.c. ~2 Hz). Moreover, the actual closure time of the valve limits the practical applicability of the technique for detecting short time constants and, hence, reduces the reliability of parameter estimates when analysing high frequencies [26]. In this regard, it should be noted that the occlusion data obtained in this study, and in others in the literature where the interruption is performed with the valve of a conventional ventilator, are affected by the finite closure time of the valve. Consequently, owing to the practical limitations arising from occluding the airway with the valve of a conventional ventilator, this technique does not allow an exploration of respiratory system mechanics for a frequency band as wide as the FOT. However, the use of a more rapidly closing valve could improve the high frequency sensitivity of the occlusion technique.

The FOT data measured from 0.25–16 Hz and their model interpretation suggest that simple models such as A, B or C (fig. 1), which are associated with a unique time constant, are not able to describe adequately the frequency dependence of R_{rs} and X_{rs} in ventilated COPD patients. By contrast, a model (D in fig. 1) featuring more than one mechanism, *i.e*. airway wall shunt and tissue viscoelasticity, significantly improved the quality of fitting (table 3, fig. 2). This model suggested that, on the one hand, the viscoelastic tissue compartment was characterized by a relatively long time constant (R_2/E_2 was 0.45 s on average, table 3) similar to that obtained from the occlusion technique (table 5). On the other hand, airway wall shunt was characterized by a much shorter time constant (~(R_1+R_p)/E_{sh}; on average ~30 ms; table 5) explaining the frequency dependence observed at high frequencies. Nevertheless, it should be noted that the fact that model D provided a reasonable description of R_{rs} and X_{rs} does not exclude the suitability of other models allowing for more than one time constant, *e.g*. models that, as expected in ventilated COPD patients, include parallel inhomogeneities [19, 20] in addition to airway wall shunting and tissue viscoelasticity. Consequently, the FOT applied for a frequency band such as the one in this work (0.25–16 Hz), which is wide enough to cover several time constants, is a potentially useful tool for exploring respiratory system properties in artificially ventilated COPD patients. Comparing the results of the FOT and AOT is of interest since the respiratory system is subjected to considerably different volume ex-cursions with the two techniques. Therefore, the results obtained from tidal volume excursions (AOT) and from small-amplitude FOT measurements at end-inspiratory and end-expiratory pauses could provide information about nonlinearities and may be useful in elucidating the mechanisms involved in inhomogeneous airway constriction [27, 28].

The potential clinical interest of the above results and modelling is enhanced by the fact that the two techniques are noninvasive and easily applicable with minimal disturbance of the artificial ventilation. On the one hand, the airway occlusion technique has been extensively used in the literature to analyse respiratory mechanics in ventilated healthy subjects and in patients with different pathologies. On the other hand, the interest in the forced oscillation technique for monitoring respiratory mechanics in intubated patients has recently been pointed out [29]. Its feasibility has been facilitated by the solution of the main methodological problems concerning this technique (generators capable of operating in parallel with the ventilator [7, 8, 10] and ways of overcoming the nonlinearity of the endotracheal tube [7, 30–32]. An additional feature of the forced oscillation technique is that it may provide automatic and on-line assessment of respiratory mechanics over the breathing cycle [7, 33–35]. As the forced oscillation technique allows practical assessment of respiratory mechanics over a frequency band wider than the occlusion

technique, its application in ventilated patients with chronic obstructive pulmonary disease may provide data for monitoring the patient's status and progress and, therefore, may be useful in optimizing the ventilator settings.

Acknowledgements: The authors wish to thank M.A. Rodríguez for his technical assistance.

References

1. Slutsky AS. Mechanical ventilation. ACCP consensus conference. *Chest* 1993; 104: 1833–1859.
2. Burke WC, Crooke PS III, Marcy TW, Adams AB, Marini JJ. Comparison of mathematical and mechanical models of pressure-controlled ventilation. *J Appl Physiol* 1993; 74: 922–933.
3. Marini JJ, Crooke PS III. A general mathematical model for respiratory dynamics relevant to the clinical setting. *Am Rev Respir Dis* 1993; 147: 14–24.
4. Peslin R, Felicio da Silva J, Chabot F, Duvivier C. Respiratory mechanics studied by multiple linear regression in unsedated ventilated patients. *Eur Respir J* 1992; 5: 871–878.
5. Polese G, Rossi A, Appendini L, Brandi G, Bates JHT, Brandolose R. Partitioning of respiratory mechanics in mechanically ventilated patients. *J Appl Physiol* 1991; 71: 2425–2433.
6. Similowski T, Bates JHT. Two-compartment modelling of respiratory system mechanics at low frequencies: gas redistribution or tissue rheology? *Eur Respir J* 1991; 4: 353–358.
7. Peslin R, Felicio da Silva J, Duvivier C, Chabot F. Respiratory mechanics studied by forced oscillations during artificial ventilation. *Eur Respir J* 1993; 6: 772–784.
8. Farré R, Ferrer M, Rotger M, Navajas D. Servocontrolled generator to measure respiratory impedance from 0.25 to 26 Hz in ventilated patients at different PEEP levels. *Eur Respir J* 1995; 8: 1222–1227.
9. Beydon L, Malassiné P, Lorino AM, *et al*. Respiratory resistance by end-inspiratory occlusion and forced oscillations in intubated patients. *J Appl Physiol* 1996; 80: 1105–1111.
10. Navajas D, Farré R, Rotger M, Torres A. Monitoring respiratory impedance by forced oscillation in mechanically ventilated patients. *Eur Respir Rev* 1994; 4: 216–218.
11. D'Angelo E, Calderini E, Torri G, Robatto FM, Bono D, Milic-Emili J. Respiratory mechanics in anesthetized paralyzed humans: effects of flow, volume and time. *J Appl Physiol* 1989; 67: 2556–2564.
12. D'Angelo E, Robatto FM, Calderini E, *et al*. Pulmonary and chest wall mechanics in anesthetized paralyzed humans. *J Appl Physiol* 1991; 70: 2602–2610.
13. Eissa NT, Ranieri VM, Corbeil C, *et al*. Analysis of behavior of the respiratory system in ARDS patients: effect of flow, volume, and time. *J Appl Physiol* 1991; 70: 2719–2729.
14. Bates JHT, Hunter IW, Sly PD, Okubo S, Filiatrault S, Milic-Emili J. Effect of valve closure time on the determination of respiratory resistance by flow interruption. *Med Biol Eng Comput* 1987; 25: 136–140.
15. Mead J. Contribution of compliance of airways to frequency dependence behaviour of lung. *J Appl Physiol* 1969; 26: 670–673.
16. Bates JHT, Brown, KA, Kochi T. Respiratory mechanics in the normal dog determined by expiratory flow interruption. *J Appl Physiol* 1989; 67: 2276–2285.
17. Otis AB, McKerrow CB, Bartlett RA, *et al*. Mechanical factors in distribution of pulmonary ventilation. *J Appl Physiol* 1956; 8: 427–443.
18. Bates JHT. Stochastic model of the pulmonary airway tree and its implication for bronchial responsiveness. *J Appl Physiol* 1993; 75: 2493–2499.
19. Lutchen KR, Greenstein JL, Suki B. How inhomogeneities and airway walls affect frequency dependence and separation of airway and tissue properties. *J Appl Physiol* 1996; 80: 1696–1707.
20. Lutchen KR, Gillis H. Relationship between heterogeneous changes in airway morphometry and lung resistance and elastance. *J Appl Physiol* 1997; 83: 1192–1201.
21. Lorino AM, Lorino H, Harf A. A synthesis of the Otis, Mead, and Mount mechanical respiratory models. *Respir Physiol* 1994; 97: 123–133.
22. Bates JHT, Rossi A, Milic-Emili, J. Analysis of the behavior of the respiratory system with constant inspiratory flow. *J Appl Physiol* 1985; 58: 1840–1848.
23. Bates JHT, Baconnier P, Milic-Emili, J. A theoretical analysis of interrupter technique for measuring respiratory mechanics. *J Appl Physiol* 1988; 64: 2204–2214.
24. Bates JHT, Daroczy B, Hantos Z. A comparison of interrupter and forced oscillation measurements of respiratory resistance in the dog. *J Appl Physiol* 1992; 72: 46–52.
25. Navajas D, Farré R, Canet J, Rotger M, Sanchis J. Respiratory input impedance in anesthetized paralysed patients. *J Appl Physiol* 1990; 69: 1372–1379.
26. Lutchen KR, Jackson AC. Reliability of parameter estima-tes from models applied to respiratory impedance data. *J Appl Physiol* 1987; 62: 403–413.
27. Suki B, Yuan H, Zheng Q, Lutchen KR. Partitioning of lung tissue response and inhomogeneous airway constriction at the airway opening. *J Appl Physiol* 1997; 82: 1349–1359.
28. Bates JHT, Schuessler TF, Dolman C, Eidelman DH. Temporal dynamics of acute isovolume bronchoconstriction in the rat. *J Appl Physiol* 1997; 82: 55–62.
29. Van de Woestijne KP. The forced oscillation technique in intubated, mechanically ventilated patients. *Eur Respir J* 1993; 6: 767–769.
30. Navajas D, Farré R, Rotger M, Canet J. Recording pressure at the distal end of the endotracheal tube to measure respiratory impedance. *Eur Respir J* 1989; 2: 178–184.
31. Lorino AM, Beydon L, Mariette C, Dahan E, Lorino H. A new correction technique for measuring respiratory impedance through an endotracheal tube. *Eur Respir J* 1996; 9: 1079–1086.
32. Navalesi P, Hernandez P, Laporta D, *et al*. Influence of site of tracheal pressure measurement on *in situ* estimation of endotracheal tube resistance. *J Appl Physiol* 1995; 58: 1840–1848.
33. Vassiliou M, Peslin R, Saunier C, Duvivier C. Expiratory flow limitation during mechanical ventilation detected by the forced oscillation method. *Eur Respir J* 1996; 9: 779–786.
34. Farré R, Peslin R, Rotger M, Navajas D. Inspiratory dynamic obstruction detected by forced oscillation during CPAP. A model study. *Am J Respir Crit Care Med* 1997; 155: 952–956.
35. Farré R, Rotger M, Montserrat JM, Navajas D. A system to generate simultaneous forced oscillation and continuous positive airway pressure. *Eur Respir J* 1997; 10: 1349–1353.